



# Monte Carlo investigation of S-values for $^{111}\text{In}$ radionuclide therapy

Jabbari<sup>a\*</sup>, M.<sup>a</sup>; Pandesh<sup>a</sup>, S.

<sup>a</sup> Department of Radiology Technology, School of Allied Medical Sciences  
Birjand University of Medical Sciences. Birjand, Iran

*masoudjabari@yahoo.com*

---

## ABSTRACT

Novel therapeutic strategy in radionuclide therapy use cell-penetrating monoclonal antibodies to carry Auger-emitting radionuclides into the cells. Estimation of dose in normal and tumor cells are important to investigate the efficacy and toxicity of treatment. Monte Carlo simulation is the most suitable method for estimation of absorbed dose at microscopic level. It is therefore useful to carry out Monte Carlo simulation of Auger emitting radionuclides in order to assess the sensitivity of the results with respect to transport approximations generally used in Monte Carlo codes. There are several Auger emitting radionuclides with potential clinical applications, however, based on their half-life  $^{111}\text{In}$  is the most suitable for Auger therapeutic purposes and was considered in the present investigation. Geant4 Monte Carlo simulation was performed and specific absorbed dose fraction (or S-values) for  $^{111}\text{In}$  were calculated by using different physics model (Standard, Livermore, Penelope and Geant4-DNA) and compared with Medical Internal Radiation Dosimetry (MIRD) S-values. Source was distributed in the cytoplasm (Cy), surface (Cs) and nucleus (N). Average of relative differences (RD) (%) were calculated for self and cross absorbed dose. RD(%) for self-absorption ( $\text{N} \leftarrow \text{N}$ ) were 4.4, 2.36, 6.21 and 1.1 for Standard, Penelope, Livermore and Geant4-DNA respectively. For cross-absorption these values were higher (e.g. for  $\text{N} \leftarrow \text{Cy}$  15.4, 18.36, 19.21 and 24.8 for Standard, Penelope, Livermore and Geant4-DNA respectively). Cutoff energy considered for electrons and gamma photons affect the results in dose estimation for Auger electrons in Monte Carlo simulation.

**Keywords:**  $^{111}\text{In}$ , Geant4, cellular S-values, MIRD.

---



## 1. INTRODUCTION

Ionizing radiation has a crucial role in the treatment of the cancer diseases. It is used both as a local field and a systemic modality. Conventionally external beams of radiation are used to explicitly expose large solid tumors recognized in the patient's body. However, it is very hard to precisely target small and disseminated tumors with external beams of radiation. When dealing with the small tumors such as breast and prostate micrometastases, systemic treatment is the only option available [1].

Systemic radiation therapy at present, confine to radionuclide therapy in which particle emitting radionuclides (mainly  $\beta$ -emitters) are attached to tumor-seeking agents in order to target the cancer cells [2]. Monoclonal antibodies are practically the most specific targeting agent available and are used in radioimmunotherapy, an advanced form of radionuclide therapy [3]. Majority of available monoclonal antibodies, target the antigens at the cell-surface and normally do not pass through intact cellular or subcellular membranes in living cells [4]. While the most susceptible part of the cells to radiation damage i.e. DNA, is located in cell nuclei. During the last two decades, there has been significant progress in production of new monoclonal antibodies and recently cell-penetrating monoclonal antibodies are under development [5]. It suggests, a novel therapeutic strategy in radionuclide therapy using cell-penetrating monoclonal antibodies to carry Auger-emitting radionuclides into the cells. Cell-penetrating pharmaceutical agents and very short range particles (i.e. Auger electrons) exclusively expose the nucleus of the target cells. The dense shower of short-range Auger electrons and highly localized energy deposited around the decay site can be very toxic to targeted cells with minor cross radiation to surrounding normal tissues [6]. The ratio of self-dose to cross radiation and therefore biological response however, will depend upon the intercellular localization of Auger-emitting radionuclides (cytoplasm, nucleus). There are several Auger emitting radionuclides e.g.  $^{111}\text{In}$  ( $t_{1/2}$ , 2.1 d),  $^{123}\text{I}$  ( $t_{1/2}$ , 13.3 h), and  $^{125}\text{I}$  ( $t_{1/2}$ , 60.5 d) with potential clinical applications, however, based on their half-life  $^{111}\text{In}$  is the most suitable for Auger therapeutic purposes and was considered in the present investigation.

Experimental dosimetry at this level is almost impossible and the only options available are analytical and Monte Carlo calculations. One of the first attempt in analytical calculation of dosimetric characteristics of auger electron performed by Medical Internal Radiation Dose (MIRD) committee of the American society of nuclear medicine [7]. However, it is very hard to consider all the transport characteristics of charged particles such as energy-loss straggling and secondary electron production in analytical calculations [8-9].

Monte Carlo is a stochastic method for solving complex, mathematical, statistical, and physical problems including the transport of particles in nonhomogeneous materials. Knowledge of the stochastic interactions of particles with matter is essential for estimation of the particle energy loss and absorbed energy to the materials along the particle's track [10]. Therefore, by evident limitation of analytical methods, Monte Carlo is the most suitable methods for estimation of absorbed dose at microscopic level. Variety of Monte Carlo codes with various degrees of sophistication in tracking the particle transport are available and have been used for cellular dosimetry [11]. An exact dose estimation requires considering the detailed spectra of radiation and exact relative abundance of the radiations emitting from the radionuclides. It is therefore useful to carry out Monte Carlo simulation of Auger emitting radionuclides in order to assess the sensitivity of the results with respect to transport approximations generally used in Monte Carlo codes.

In this study, we used Evaluated Nuclear Data File (ENDF/B-IV) cross-sections to establish S values of  $^{111}\text{In}$  to the nucleus for a single cell and report in 36 situation cell model that contain two nested spheres in 5-12 and 2-11 micrometers as cell and nucleus radius respectively. Geant4 Monte Carlo simulation was performed and S-values for  $^{111}\text{In}$  were calculated by using different physics model (Standard, Livermore, Penelope and Geant4-DNA) and compared with MIRD S-values.

## **2. MATERIALS AND METHODS**

### **2.1. GEANT4 Monte Carlo code**

We used Geant4 (Geant4.11.0.patch02) as the Monte Carlo simulator [12]. It includes several C++ class libraries that provide functions for all types of electromagnetic processes. It provides 4

physics models to choose based on the energy of particles including: standard, low-energy Penelope, low-energy Livermore and very low-energy Geant4-DNA. They can cover electron interaction down to 1 keV, 250 eV, 250 eV and 10 eV for standard, Penelope, Livermore and DNA models.

In all simulations, photoelectric effect, Compton interaction and Rayleigh scattering were considered for photon transport. For electron transport, bremsstrahlung interaction, atomic ionization and atomic scattering were considered. Auger electron and x-ray production were also activated in all simulations. Simulations were performed on a PC (Intel® Core™ i7 Processors) operating on Linux fedora 19. We performed 6 simulations simultaneously on different cores. No variance-reduction method was used in the simulations.

## 2.2. Decay scheme of $^{111}\text{In}$

Radiation emitting from  $^{111}\text{In}$  were set exactly based on MIRD: Radionuclide Data and Decay Schemes [13]. Radionuclide  $^{111}\text{In}$  decays by electron capture (100%) and each nuclear transition results in 13 Auger electrons with mean energy  $E_m=0.926$  keV and the total yield of  $Y_r=7.431$ . The decay scheme also includes 12 conversion electrons ( $E_m=176.100$  keV,  $Y_r=0.158$ ), 42 low energy x-ray photons ( $E_m=2.105$  keV,  $Y_r=9.498$ ) and 2 gamma photons ( $E_m=209.000$ , keV,  $Y_r=1.847$ ). As per GEANT4 procedure; each type of radiation was defined using a discrete histogram (his point spectrum) at the energy resolution of 1 eV. The relative yields reported in MIRD was assumed to be significant up to 3 decimal number. (Figures 1)

## 2.3. Geometry of simulation for S-values

The cell model used for the present calculations consisted of two nested spheres as cells and its nucleus. The radius of the cell and nucleus ranged from 5 to 12 mm and 2 to 11 mm, respectively. This cell sizes were selected in order to compare the results with published data [14]. As in other papers published we assumed the cells are composed of unit density water (G4\_WATER) [15]. Radionuclide [ $^{111}\text{In}$ ] was assumed to be uniformly distributed in one of the following regions and simulation was performed independently; inside the cytoplasm (Cy), over the cell surface (CS), and inside the cell nucleus (N). In each simulation  $10^4$  decays was considered and the absorbed energy

in target region ( $r_k$ ) from the radiation in source organs ( $r_h$ ) was determined. Based on the MIRD schema the corresponding s-values were calculated.

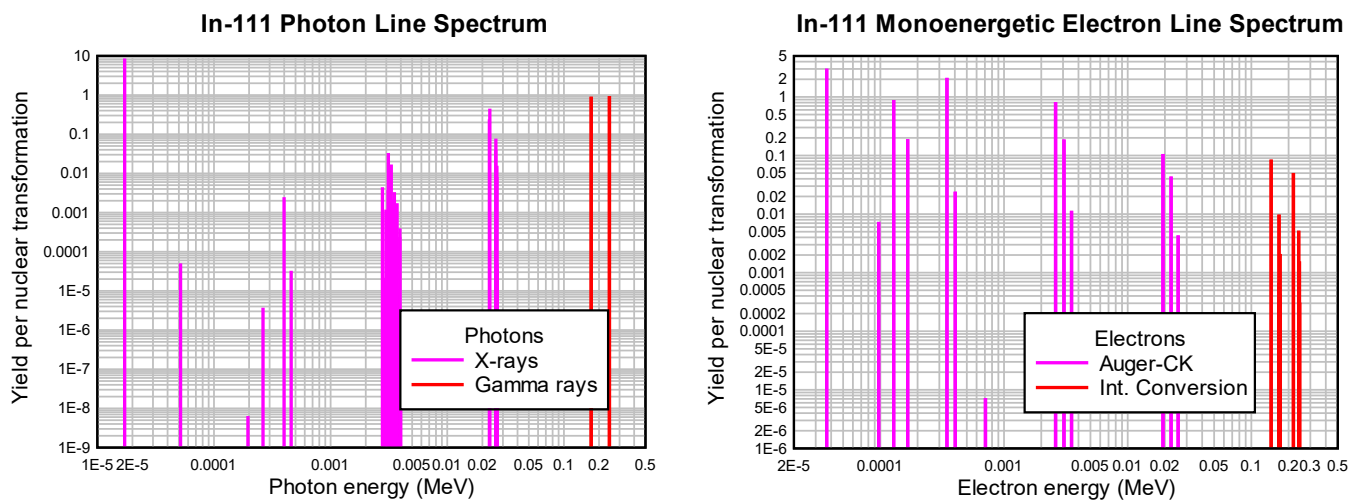
### 2.4. Data analyses

They only considered conversion electrons (145–245 keV) and Auger electrons (8.5 eV- 25.5 keV) released during  $^{111}\text{In}$  decay for dose calculation. They considered  $10^4$  electrons history to achieve standard deviations (or uncertainty) smaller than 1%. The energy cut-off was 1 keV that is the electrons energy lower than 1 keV was assumed locally absorbed in the spot. Relative differences (RD) in percent were calculated according to the following formula:

$$\text{RD \%} = \frac{S_D - S_H}{S_H} \times 100$$

Where  $S_D$  and  $S_H$  represent the S-values calculated using Monte Carlo and MIRD respectively.

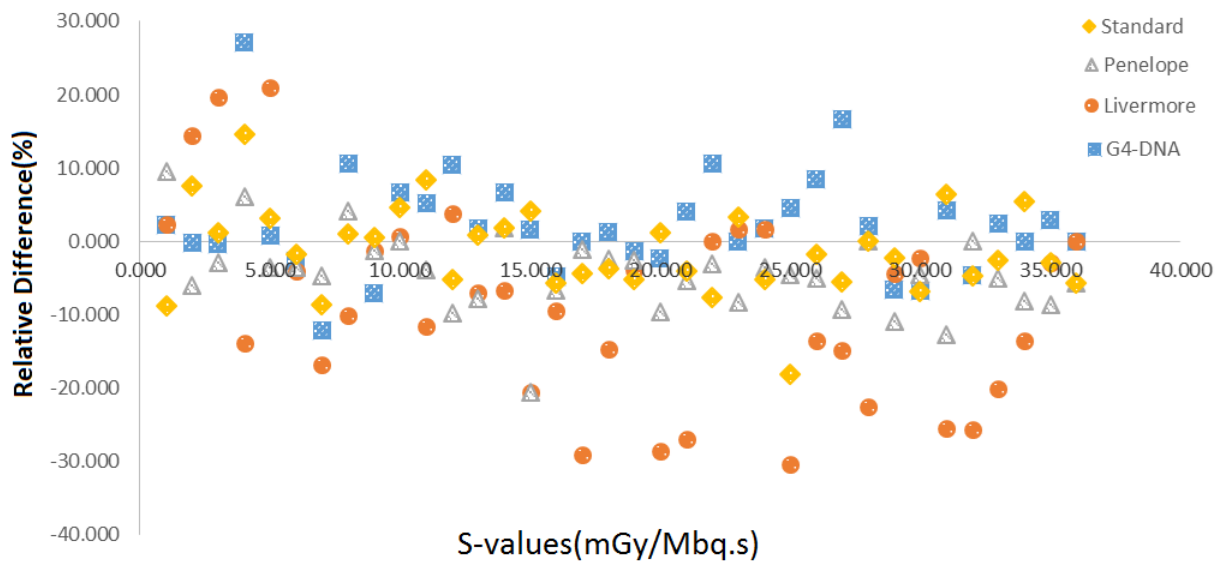
**Figure 1.** *The Spectrum of In-111 radiation*



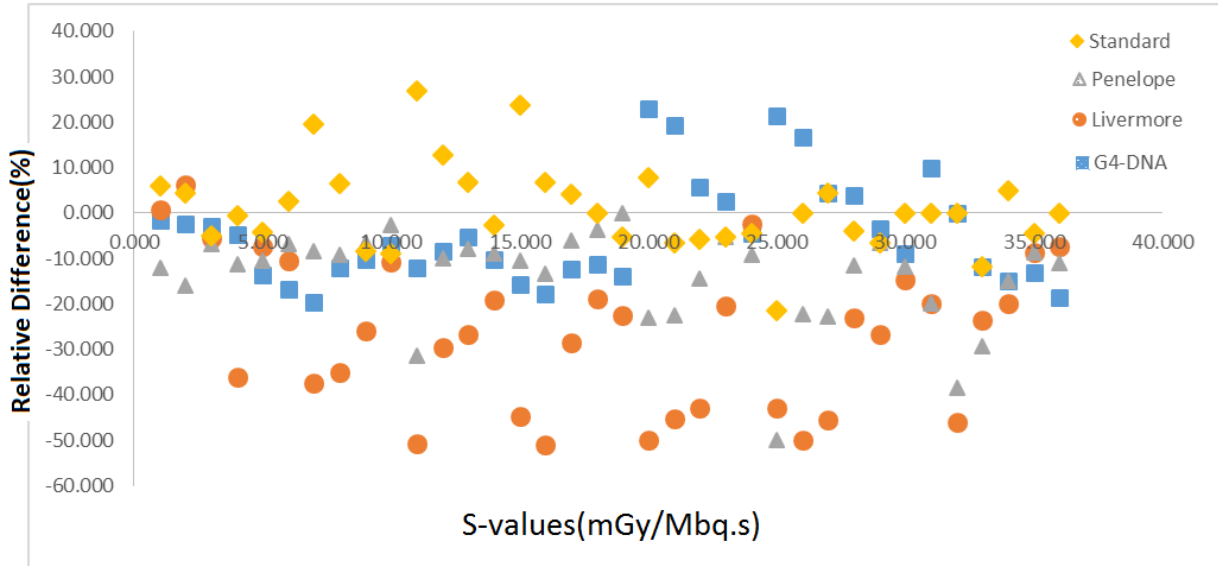
### 3. RESULTS AND DISCUSSION

Figures 2-5 includes the scatter plot of the relative difference between four series of data. This figure demonstrates the Bland-Altman plot to reveal the RD versus reference values (MIRD S-values). Relative differences are up to 11.46% for self-absorption but higher (36.34%) for cross-absorption. The average value of relative differences named bias demonstrates a systematic difference in Monte Carlo simulation. As the plot shows although 85% of the data points are inside the limits of agreement (average of RD  $\pm$  1.96  $\times$  standard deviation of RD) and the statistical difference is acceptable ( $\approx$ 5%) but there is a high bias (5.27%) between data.

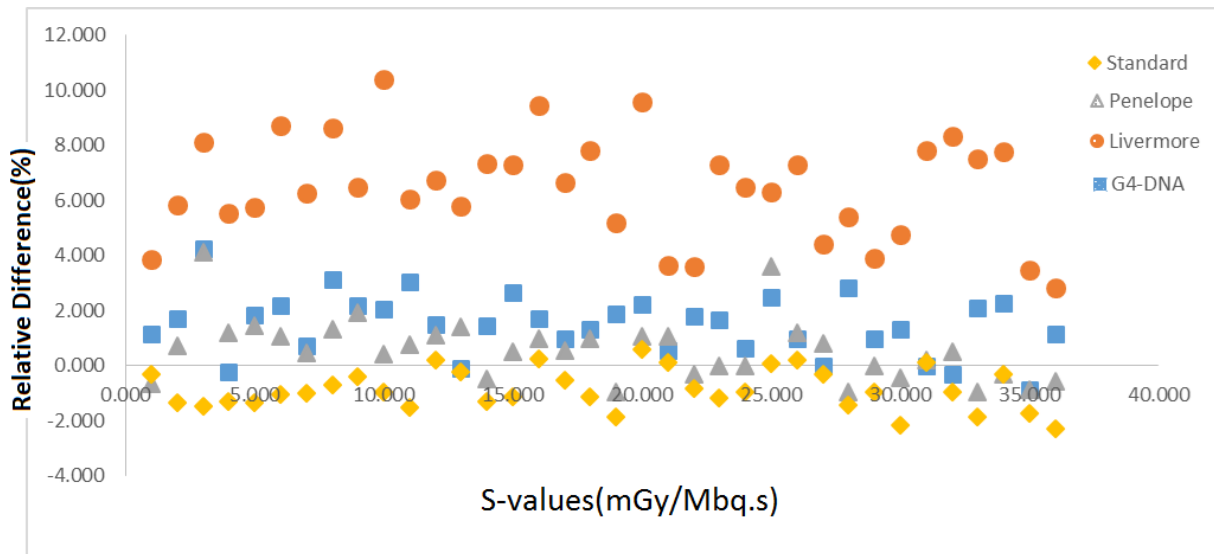
**Figure 2:** *S-value  $S(N \leftarrow Cy)$  difference percent based MIRD*

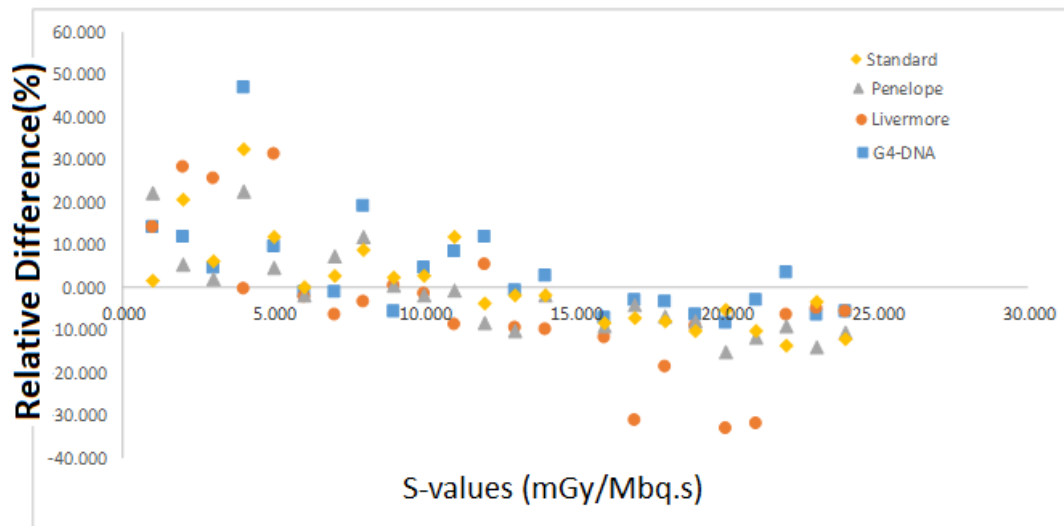


**Figure 3:**  $S$ -value  $S(N \leftarrow Cs)$  difference percent based MIRD



**Figure 4:**  $S$ -value  $S(N \leftarrow N)$  difference percent based MIRD



**Figure 5:**  $S$ -value  $S(N \leftarrow Cy)$  difference percent based MIRD

#### 4. CONCLUSIONS

Radionuclide therapy has the potential to restrict the radiation exposure to the target cells with minimum impact to the surrounding normal tissues [16]. However, to achieve this advantage accurate targeting of the cancer cells and short range  $\beta$ -particles are essential [17].

Consequently, for maximum cell toxicity, an exact balance between the average radius of target cells and the effective range of the  $\beta$ -particles is necessary [18]. If particle range is too short, absorbed dose to DNA may not sufficient to eradicate the targeted cells. If range of the particles is too long, neighboring cells will also be under radiation exposure. This cross radiation may be useful in treatment of large solid tumors however, in micrometastases tumors, cross radiation may cause damage to surrounding normal tissues. Establishing the required balance is a difficult task in clinical practice because of multiplex spectrum of  $\beta$ -particles and complex geometry of micrometastases [19].

The energy of Auger electrons are very low (1 eV to 20 keV) and their ranges in tissue is short below micrometer [20]. Accurate dose estimation for Auger electrons thus requires spatial resolution at subcellular level comparable to the size of a DNA molecules.



Most of the general-purpose Monte Carlo codes available for radiation transport (EGS, MCNP, PENELOPE and GEANT4 ) are developed based on condensed history technique in which, the particle's track are divide into small segments and the energy transferred along the segments and the scatter angle at the end of segments are stochastically determined [21-22]. Some dedicated codes were also developed based on the track structure technique wherein simulation is performed for all the collisions in an event-by-event manner [23]. These codes are probably more suitable for Auger electron dosimetry however, most of them are in-house codes and not freely available, an exception is the GEANT4-DNA track-structure physics an available option with GEANT4 [24].

There are many reports on estimation of Auger-emitting radionuclides dose point kernels and corresponding absorbed doses at sub-cellular levels with some degree of inconsistency in their results [25-27]. Usually, the discrepancies are referred to different cross-section tables used and different physical models implemented to describe the interactions in the codes [28]. However, in most of the studies some important issues were generally overlooked. One factor that influences the results of Auger dosimetry is the accompanying radiation with Auger emission. Auger electrons are released as a consequence of radionuclides decay via electron capture (e.g.  $^{111}\text{In}$ ,  $^{123}\text{I}$ ,  $^{125}\text{I}$ ) or isomeric transition ( $^{99\text{m}}\text{Tc}$ ). In both cases, emission of gamma photons is possible. Internal conversion and emission of conversion electrons is common after electron capture and isomeric transition. Along with Auger electrons, low-energy x-rays are always released. All these concomitant particles can ionize the surrounding atoms and produce secondary  $\delta$ -electrons at different distances from the point of disintegration that in turn may release tertiary Auger and x-ray photons.

In many studies, low abundance radiations are ignored and the average energy is sometimes used for multiple energy particles. Moreover, there is no agreement about the standard database to access the decay scheme of radionuclides. Conventionally, investigators in different fields use different databases to access decay schemes or radionuclides. Another factor that may affect the results is the cutoff energy considered for electrons and gamma photons. In Auger electron simulation, a very low-energy cutoff is necessary while in many Monte Carlo codes sub-keV cutoff is meaningless. Geant4-DNA ability to simulation of electron interaction down to sub eV (11 eV for ionization) is an important factor especially for Auger emitting electron dosimetry. Good

conformity observed in comparison but the difference back to collision stopping power used by MIRD (used analytical stopping power by Cole-Howell) and negligibility of  $\delta$ -ray straggling.

## . REFERENCES

- [1] Müller V, Stahmann N, Riethdorf S, Rau T, Zabel T, Goetz A, Jänicke F, Pantel K. Circulating tumor cells in breast cancer: correlation to bone marrow micrometastases, heterogeneous response to systemic therapy and low proliferative activity. *Clinical Cancer Research*. 2005 May 15;11(10):3678-85.
- [2] Goldenberg DM. Targeted therapy of cancer with radiolabeled antibodies. *Journal of Nuclear Medicine*. 2002 May 1;43(5):693-713.
- [3] Jain M, Venkatraman G, Batra SK. Optimization of radioimmunotherapy of solid tumors: biological impediments and their modulation. *Clinical cancer research*. 2007 Mar 1;13(5):1374-82.
- [4] Koren E, Torchilin VP. Cell-penetrating peptides: breaking through to the other side. *Trends in molecular medicine*. 2012 Jul 1;18(7):385-93.
- [5] Thomas S, Hoxha K, Alexander W, Gilligan J, Dilbarova R, Whittaker K, Kossenkov A, Prendergast GC, Mullin JM. Intestinal barrier tightening by a cell-penetrating antibody to Bin1, a candidate target for immunotherapy of ulcerative colitis. *Journal of Cellular Biochemistry*. 2019 Mar;120(3):4225-37.
- [6] Aghevlian S, Boyle AJ, Reilly RM. Radioimmunotherapy of cancer with high linear energy transfer (LET) radiation delivered by radionuclides emitting  $\alpha$ -particles or Auger electrons. *Advanced drug delivery reviews*. 2017 Jan 15;109:102-18.
- [7] Bolch WE, Eckerman KF, Sgouros G, Thomas SR. MIRD pamphlet no. 21: a generalized schema for radiopharmaceutical dosimetry—standardization of nomenclature. *Journal of Nuclear Medicine*. 2009 Mar 1;50(3):477-84.
- [8] Makrigiorgos GM, Adelstein SJ, Kassis AI. Limitations of conventional internal dosimetry at the cellular level. *Journal of nuclear medicine*. 1989 Nov 1;30(11):1856-64.
- [9] Bousis C, Emfietzoglou D, Hadjidoukas P, Nikjoo H. Monte Carlo single-cell dosimetry of Auger-electron emitting radionuclides. *Physics in Medicine & Biology*. 2010 Apr 14;55(9):2555.
- [10] Bousis C, Emfietzoglou D, Nikjoo H. Monte Carlo single-cell dosimetry of I-131, I-125 and I-123 for targeted radioimmunotherapy of B-cell lymphoma. *International journal of radiation biology*. 2012 Dec 1;88(12):908-15.

- [11] Cai Z, Pignol JP, Chan C, Reilly RM. Cellular dosimetry of  $^{111}\text{In}$  using Monte Carlo N-particle computer code: comparison with analytic methods and correlation with in vitro cytotoxicity. *Journal of Nuclear Medicine*. 2010 Mar 1;51(3):462-70.
- [12] Agostinelli S, Allison J, Amako KA, Apostolakis J, Araujo H, Arce P, Asai M, Axen D, Banerjee S, Barrand GJ, Behner F. GEANT4—a simulation toolkit. *Nuclear instruments and methods in physics research section A: Accelerators, Spectrometers, Detectors and Associated Equipment*. 2003 Jul 1;506(3):250-303.
- [13] Eckerman KF, Endo A. MIRD: radionuclide data and decay schemes. *Snmmi*; 2007.
- [14] Bousis C, Emfietzoglou D, Hadjidoukas P, Nikjoo H. Monte Carlo single-cell dosimetry of Auger-electron emitting radionuclides. *Physics in Medicine & Biology*. 2010 Apr 14;55(9):2555.
- [15] Incerti S, Ivanchenko A, Karamitros M, Mantero A, Moretto P, Tran HN, Mascialino B, Champion C, Ivanchenko VN, Bernal MA, Francis Z. Comparison of GEANT4 very low energy cross section models with experimental data in water. *Medical physics*. 2010 Sep;37(9):4692-708.
- [16] Dash A, F Russ Knapp F, Ra Pillai M. Targeted radionuclide therapy-an overview. *Current radiopharmaceuticals*. 2013 Sep 1;6(3):152-80.
- [17] Bodei L, Kassis AI, Adelstein SJ, Mariani G. Radionuclide therapy with iodine-125 and other auger–electron-emitting radionuclides: Experimental models and clinical applications. *Cancer Biotherapy and Radiopharmaceuticals*. 2003 Dec 1;18(6):861-77.
- [18] Behr TM, Béhé M, Löhr M, Sgouros G, Angerstein C, Wehrmann E, et al. Therapeutic advantages of Auger electron-over beta-emitting radiometals or radioiodine when conjugated to internalizing antibodies. *Eur J Nucl Med*. 2000;27:753–65.
- [19] Tamborino G, Saint-Hubert D, Struelens L, Seoane DC, Ruigrok EA, Aerts A, van Cappellen WA, de Jong M, Konijnenberg MW, Nonnekens J. Cellular dosimetry of [ $^{177}\text{Lu}$ ] Lu-DOTA-[Tyr3] octreotate radionuclide therapy: the impact of modeling assumptions on the correlation with in vitro cytotoxicity. *EJNMMI physics*. 2020 Dec;7(1):1-9.
- [20] Cai Z, Kwon YL, Reilly RM. Monte Carlo N-particle (MCNP) modeling of the cellular dosimetry of  $^{64}\text{Cu}$ : comparison with MIRDcell S values and implications for studies of its cytotoxic effects. *Journal of Nuclear Medicine*. 2017 Feb 1;58(2):339-45.
- [21] Salim R, Taherparvar P. Monte Carlo single-cell dosimetry using Geant4-DNA: the effects of cell nucleus displacement and rotation on cellular S values. *Radiation and Environmental Biophysics*. 2019 Aug;58(3):353-71.

[22] Syme AM, Kirkby C, Riauka TA, Fallone BG, McQuarrie SA. Monte Carlo investigation of single cell beta dosimetry for intraperitoneal radionuclide therapy. *Physics in Medicine & Biology*. 2004 May 4;49(10):1959.

[23] Uusijärvi H, Chouin N, Bernhardt P, Ferrer L, Bardies M, Forssell-Aronsson E. Comparison of electron dose-point kernels in water generated by the Monte Carlo codes, PENELOPE, GEANT4, MCNPX, and ETRAN. *Cancer biotherapy and radiopharmaceuticals*. 2009 Aug 1;24(4):461-7.

[24] André T, Morini F, Karamitros M, Delorme R, Le Loirec C, Campos L, Champion C, Groetz JE, Fromm M, Bordage MC, Perrot Y. Comparison of Geant4-DNA simulation of S-values with other Monte Carlo codes. *Nuclear Instruments and Methods in Physics Research Section B: Beam Interactions with Materials and Atoms*. 2014 Jan 15;319:87-94.

[25] Thisgaard H, Olsen BB, Dam JH, Bollen P, Mollenhauer J, Høiland-Carlsen PF. Evaluation of Cobalt-Labeled Octreotide Analogs for Molecular Imaging and Auger Electron-Based Radionuclide Therapy. *Journal of Nuclear Medicine*. 2014 Aug 1;55(8):1311-6.

[26] Bastami H, Chiniforush TA, Heidari S, Sadeghi M. Dose evaluation of auger electrons emitted from the  $^{119}\text{Sb}$  in cancer treatment. *Applied Radiation and Isotopes*. 2022 Jul 1;185:110250.

[27] Salim R, Taherparvar P. Dosimetry assessment of theranostic Auger-emitting radionuclides in a micron-sized multicellular cluster model: A Monte Carlo study using Geant4-DNA simulations. *Applied Radiation and Isotopes*. 2022 Oct 1;188:110380.

[28] Villagrasa C, Rabus H, Baiocco G, Perrot Y, Parisi A, Struelens L, Qiu R, Beuve M, Poignant F, Pietrzak M, Nettelbeck H. Intercomparison of micro-and nanodosimetry Monte Carlo simulations: An approach to assess the influence of different cross-sections for low-energy electrons on the dispersion of results. *Radiation Measurements*. 2022 Jan 1;150:106675.

This article is licensed under a Creative Commons Attribution 4.0 International License, which permits use, sharing, adaptation, distribution and reproduction in any medium or format, as long as you give appropriate credit to the original author(s) and the source, provide a link to the Creative Commons license, and indicate if changes were made. The images or other third-party material in this article are included in the article's Creative Commons license, unless indicated otherwise in a credit line to the material.

To view a copy of this license, visit <http://creativecommons.org/licenses/by/4.0/>.